Published in final edited form as:
J Am Chem Soc. 2009 October 28; 131(42): 15317–15329. doi:10.1021/ja9056008.

Enzymatic Tailoring of Ornithine in the Biosynthesis of the *Rhizobium* Cyclic Trihydroxamate Siderophore Vicibactin

John R. Heemstra Jr., **Christopher T. Walsh***, and **Elizabeth S. Sattely**
Department of Biological Chemistry and Molecular Pharmacology, Harvard Medical School, Boston, Massachusetts 02115

Abstract

To acquire iron, the N_2-fixing, symbiotic bacterium *Rhizobium sp.* produce the cyclic tri-hydroxamate siderophore vicibactin, containing a 30-membered tri-lactone scaffold. Herein we report the overproduction and purification of the six proteins VbsACGOLS in the bacterial host *Escherichia coli* and the reconstitution of the biosynthesis of vicibactin from primary metabolites. The flavoprotein VbsO acts as a pathway-initiating L-ornithine N^5-hydroxylase, followed by VbsA which transfers (*R*)-3-hydroxybutyryl- from the CoA thioester to N^5-hydroxyornithine to yield N^5-((*R*)-3-hydroxybutyryl)-N^5-hydroxy-L-ornithine. VbsL is a PLP-dependent epimerase acting at C^2 of the 10 atom monomer unit. VbsS, a nonribosomal peptide synthetase free standing module, then activates N^5-((*R*)-3-hydroxybutyryl)-N^5-hydroxy-D-ornithine as the AMP anhydride on the way to cyclotrimerization to the vicibactin scaffold. The last step, tris-acetylation of the C^2 amino group of desacetyl-D-vicibactin to the mature siderophore vicibactin is catalyzed distributively by VbsC, using three molecules of acetyl-CoA.

Introduction

Iron is required for growth of nearly all living organisms.[1] To cope with the often limited availability of soluble iron in microenvironments, bacteria and fungi[2] maintain a branch of secondary metabolism for the production of Fe(III)-scavenging small molecule siderophores. In response to iron starvation, these microbes turn on genes that encode for the biosynthesis[3] and export of apo-siderophores and also for the uptake and accumulation of the iron-loaded forms.[1] Siderophores are commonly made up of peptides decorated with iron-chelating functionality of four main classes: (1) phenols and catechols, (2) heterocyclic oxazolines and thiazolines, (3) hydroxamates, and (4) the α-hydroxyl-carboxylates.[1,4]

The dominant logic for the biosynthesis of phenolic and catecholic siderophores such as enterobactin[5] involves amine acylation, while heterocycles such as the thiazolines of yersiniabactin[6] and pyochelin[7] are derived from modified cysteine or serine residues. Each of these tailoring events is known to occur through the action of nonribosomal peptide synthetase (NRPS) assembly lines.[8] Hydroxamates also appear to originate from primary metabolic precursors, for example ornithine and lysine; however, the pathway for elaboration to the mature hydroxamate-containing siderophore is not as obvious.

Despite the structural similarities of fungal fusarinines,[9,10] bacterial vicibactins,[11,12] and desferrioxamines[13] exemplified in Figure 1, two parallel strategies appear to have evolved for

christopher_walsh@hms.harvard.edu.

Supporting Information Available. Figures S1-S19, Table S1, detailed experimental procedures and spectroscopic data for the preparation of compounds **3** and **9**. This material is available free of charge via the Internet at http://pubs.acs.org.

the biosynthesis of these related hydroxamate siderophores. While each macrocycle consists of a trimerized monomer, it is thought that different classes of ATP-dependent synthetases are generally utilized for the synthesis of ester verses amide-containing siderophores.[14] For example, in desferrioxamine E production by *Streptomyces coelicolor*, the enzyme DesD uses ATP to activate *N*-hydroxy-*N*-succinylcadaverine units as the mixed anhydride (with release of PPi) and catalyzes trimerization of soluble intermediates through a stepwise mechanism[15] to generate the 33-membered macrocyclic triamide.[16] In contrast, the pathogenic mold *Aspergillus fumigatus* makes virulence-related siderophores fusarinine C and the triacetylfusarinine C derivative as 36–membered marocyclic trilactones (depsipeptide).[17] The fusarinine C scaffold is assembled by the action of the multidomain nonribosomal peptide synthetase SidD that also utilizes ATP-dependent substrate activation. Rather than linking soluble monomers as in the case of DesD, the fusarinine mechanism for trimerization is thought to occur through the successive condensation of N^5-*cis*-anhydromevalonyl-N^5-hydroxy-L-ornithine covalently templated on the pantetheinyl arm of the synthetase thiolation domain.

Several chemical steps are required to transform an amine-containing metabolite to an iron-chelating hydroxamic acid. In the context of global strategies for siderophore biosynthesis, we have been interested in the timing of biological *N*-oxygenation verses *N*-acylation and the fate of the resulting hydroxamate, including cyclotrimerization to trilactone macrocyclic scaffolds. A close relative to the *A. fumigatus* siderophore fusarinine is the trihydroxamate vicibactin,[18,19] produced by the N_2-fixing, pea symbiotic bacterium *Rhizobium leguminosarum*.[20] Although both siderophores are derived from similarly elaborated monomers, vicibactin harbors an additional degree of complexity in the D-isomer of Orn. In addition, the core vicibactin NRPS, VbsS,[11] presumably responsible for the assembly of the 30-membered trilactone, has a distinct domain organization that differs markedly from the fungal assembly line SidD. Following trimerization of N^5-((*R*)-3-hydroxybutyryl)-N^5-hydroxy-D-ornithine, presumably activated as the phosphopantetheinyl thioester on VbsS, the macrocyclic scaffold is further tailored through three-fold *N*-acetylation at the N^2-amino groups. It is possible that this final modification helps to curtail unwanted acyl transfer reactions or to block the association of positive charge with the mature siderophore. Despite the suggested role and known requirement of VbsS in vicibactin assembly,[11] details of the timing and mechanism of monomer provision are not known.

The nitrogen-fixing ability of *Rhizobia sp*. has enabled use of these microbes as “biofertilizers”,[21] especially for leguminous plants. In return for a source of usable nitrogen, plants provide root nodules and nutrients for *Rhizobia* colonization.[22] The multiple FeS clusters essential to endogenous nitrogenase catalysis[23] presents *Rhizobia* with a particular need for iron accumulation. It has been observed that vicibactin-mediated collection of iron from the rhizosphere is an important determinant of productive symbiosis.[24]

In 2002 Carter[11] and coworkers identified a cluster of eight genes for vicibactin biosynthesis synthesis, *vbsGSO, vbsADL, vbsC* and *vbsP*, in *Rhizobium leguminosarum*, assigned functions by a combination of bioinformatic predictions and genetic knockouts of each of the *vbsACGLOS* genes, and proposed a pathway that features the single NRPS module protein VbsS as the central catalyst (Figure 2). Bioinformatic analysis of the fully sequenced relative *Rhizobium etli* CFN42[25] revealed the presence of an analogous gene cluster. In this study we have expressed and purified the six enzymes VbsA, C, L, O, and VbsGS from *R. etli* CFN42 in *E. coli* and have established catalytic activities that provide insights into the timing of ornithine N^5-hydroxylation and acylation, the construction of the ten atom N^5-((*R*)-3-hydroxybutyryl)-N^5-hydroxy-D-ornithine monomer unit, its activation by the adenylation (A) domain of the four domain (C-A-T-TE) VbsS NRPS single module subunit, and the tris-acetylation at N^2 of desacetyl-D-vicibactin.

Materials and Methods

Standard recombinant DNA, molecular cloning, and microbiological procedures were performed according to the methods described by Sambrook *et al*.[26] *E. coli* Top10 (Invitrogen) was used for routine cloning and propagation of DNA vectors. *E. coli* BL21 (DE3) (Invitrogen) transformed with pET-derived vectors (Novagen) was used for overexpression in Luria-Bertani (LB) medium supplemented with kanamycin. Oligonucleotide primers were synthesized by Integrated DNA Technologies (Coralville, IA). Phusion DNA polymerase, restriction enzymes, and T4 DNA ligase were purchased from New England Biolabs. Recombinant plasmid DNA was purified with a Qiaprep kit from Qiagen. Gel extraction of DNA fragments and restriction endonuclease cleanup was done with a QIAquick PCR cleanup kit from Qiagen. DNA sequencing was performed at the Molecular Biology Core Facilities of the Dana Farber Cancer Institute (Boston, MA). Nickel-nitrilotriacetic acid-agarose (Ni-NTA) superflow resin and SDS-page gels were purchased from Biorad. Protein samples were concentrated using 10K mwco Amicon Ultra filters from Millipore.

HPLC analysis was performed on a Beckman System Gold (Beckman Coulter) instrument on a Supleco Discovery C18 column (250 × 4.6 mm). MS analysis of samples was carried out on an Agilent 6210 Time-of-Flight MS with a dual nebulizer ESI source. ^{1}H NMR spectra were recorded on a Varian 600 MHz spectrometer. Chemical shifts are reported in ppm from tetramethylsilane with the solvent resonance resulting from incomplete deuteration as the internal standard ($CDCl_3$ δ 7.26, D_2O δ 4.75). Data are reported as follows: chemical shift, multiplicity (s = singlet, d = doublet, t = triplet, q = quartet, br = broad, m = multiplet), coupling constants (Hz), and integration. A Cary 50 Bio scanning spectrometer was employed to record absorption spectra. Details for synthetic substrate preparations are included in the supporting information.

Cloning, Overexpression, and Purification of VbsO, VbsA, VbsL and VbsC

The *vbsO*, *vbsA*, *vbsL* and *vbsC* genes of the vicibactin cluster were individually obtained by PCR amplification with Phusion DNA polymerase of genomic DNA isolated from *Rhizobium etli* CFN42 (ATCC51251). The *vbsO* gene was PCR amplified using the forward primer 5′-aatcaatcatatgaccgtcgcttttacccgc-3′ (*Nde*I restriction site underlined) and reverse primer 5′-gatcaagcttggacgagagcatgccgtc-3′ (*Hin*dIII restriction site underlined). The *vbsA* gene was PCR amplified using the forward primer 5′-aatcaatcatatggatttcgatgccgccaga-3′ (*Nde*I restriction site underlined) and reverse primer 5′-gatcaagctttcatgatgccggcacccagag-3′ (*Hin*dIII restriction site underlined). The *vbsL* gene was PCR amplified using the forward primer 5′-aatcaatcatatgaaccagtccttcagcccc-3′ (*Nde*I restriction site underlined) and reverse primer 5′-gatcaagctttcaccgcttcgcggcgtgcag-3′ (*Hin*dIII restriction site underlined). The *vbsC* gene was PCR amplified using the forward primer 5′-aatcaatcatatgagacgaacagtcgagatt-3′ (*Nde*I restriction site underlined) and reverse primer 5′-gatcaagctttcaaagcgcggtcctgctcag-3′ (*Hin*dIII restriction site underlined). The purified PCR products were digested with *Nde*I and *Hin*dIII, ligated into similarly digested pET24b (*vbsO*) or pET28a (*vbsA*, *vbsL*, and *vbsC*) expression vectors using T4 DNA ligase (New England Biolabs). The recombinant plasmids were propagated in *E. coli* TOP10 cells and the identity of the resulting pET-24b (C-His_6) and pET-28a (N-His_6) constructs were confirmed by DNA sequencing. The expression constructs were used to transform *E. coli* BL21 (DE3) cells, grown to saturation in LB medium supplemented with 50 μg/mL kanamycin at 37 °C, and diluted 1:100 into LB medium containing 50 μg/mL kanamycin. The cultures were incubated at 37 °C with shaking, induced with 100 μM IPTG at OD_{600} = 0.5–0.6, and then incubated at 15 °C for ~18h. The cells were harvested by centrifugation (6,000 rpm × 6 min), resuspended in 30 mL of lysis buffer (25 mM Tris, pH 8.0, 500 mM NaCl) and then lysed with two passes through an Emulsiflex-C5 cell disruptor (Avestin). The lysate was clarified by ultracentrifugation (35,000 rpm × 35 min). The

supernatant was incubated with Ni-NTA resin (0.25 mL/L culture, prewashed with lysis buffer) for 1 h at 4 °C, and the mixture was centrifuged (1800 rpm × 15 min). The unbound fraction was discarded, and the resin was then transferred to a column and the protein was eluted with an imidazole gradient using steps of 25 mL of 0 and 5 mM imidazole, 10 mL of 25 and 200 mM imidazole, and 5 mL of 500 mM imidazole in lysis buffer. SDS-PAGE analysis (4–15% Tris-HCl gel, BioRad) was employed to ascertain the presence and purity of protein in each fraction. Fractions containing pure protein were concentrated to 2 mL and subjected to gel filtration on a Superdex 200 column connected to an Amersham automated FPLC system at 4 °C (20 mM HEPES, pH 7.5, 80 mM NaCl, 10% glycerol was used as the eluent). Fractions containing the desired protein were concentrated with a Millipore 10 kDa MW cutoff filter, flash frozen in liquid N_2 as pellets, and stored at −80 °C. The concentration of purified protein solutions was determined by the method of Bradford,[26] with BSA as a standard (VbsO and VbsL) or spectrophotometrically using calculated extinction coefficients at (VbsA ε_{280} = 37,930 $M^{-1}cm^{-1}$ and VbsC ε_{280} = 18,479 $M^{-1}cm^{-1}$).

Cloning, Overexpression, and Purification of VbsGS

The fragment encoding *vbsGS* was subcloned from genomic DNA isolated from *Rhizobium etli* CFN42 (ATCC51251) as a bicistronic operon using the forward primer 5′-aatcaatcatatggacaatcttgagccccgc-3′ (*Nde*I restriction site underlined) and the reverse primer 5′-gatcaagctttgcgttatccttctctgt-3′ (*Hin*dIII restriction site underlined). The transcript was amplified and ligated into similarly digested pET-24b vector as described above to append a C-terminal His_6 tag to VbsS (VbsG untagged). The recombinant plasmid was propagated in *E. coli* Top10 cells and confirmed by sequencing. After transformation of *E. coli* BL21 with the *vbs*GS-containing plasmid, two 2 L cultures of the resulting expression strain were grown at 25 °C in LB media (supplemented with 40 μg/mL kanamycin) with shaking at 180 rpm to an OD_{600} of 0.3, and then at 15 °C to an OD_{600} of 0.6 at which time expression was induced by the addition of IPTG to a final concentration of 0.1 mM, and growth was continued at 15 °C for 15 h before the cells were harvested. A suspension of collected cells in lysis buffer (25 mL; 20 mM Tris, 0.5 M NaCl, pH 8) was lysed with two passes through an Emulsiflex-C5 cell disruptor (Avestin). The lysate was clarified by ultracentrifugation (35,000 rpm for 35 min), combined with $(NH_4)_2SO_4$ to a saturation of 20% at 4 °C with gentle stirring, and further incubated for 1 h. The precipitated protein was separated by ultracentrifugation (35,000 rpm for 35 min) and resuspended in 10 mL of lysis buffer at 4 °C. Gentle stirring and agitation with a spatula over 30 min was used to encourage dissolution. The resulting cloudy solution was filtered through a 45 um Acrodisc syringe filter and subjected to gel filtration on a Superdex 200 column connected to an Amersham automated FPLC system at 4 °C (20 mM Tris, 50 mM NaCl, 10% v/v glycerol, pH = 8 was used as the eluent). Fractions containing VbsS, coeluting with VbsG (as indicated by SDS PAGE analysis with Coomassie staining and in gel tryptic digest/MS sequencing), were combined, concentrated to 6 mL with a Millipore 50 kDa MW cutoff filter, flash frozen in liquid N_2 as pellets, and stored at −80 °C; concentration was determined spectrophotometrically by absorbance at 280 nm.

Assays for VbsO *N*-hydroxylase Activity

To a solution of L-ornithine or D-ornithine (500 μM), FAD (50 μM), NADPH (2 mM) and pH 8.0 Tris buffer (50 mM) at 25 °C was added VbsO (5 μM) to initiate the reaction (total reaction volume of 50 μL). After 20 min the reactions were halted with MeCN (100 μL), chilled at −20 °C for 10 min and centrifuged at 13,000 rpm for 5 min. The supernatant was withdrawn, combined with 25 μL of 200 mM borate (pH 8.0), followed by 20 μL of 10 mM 9-fluorenylmethyl chloroformate (Fmoc-Cl) and the reaction was allowed to proceed at room temperature for 5 min. To remove any remaining derivatizing reagent, 20 mL of 0.1 M 1-aminoadamantane was added and the mixture was kept at room temperature for an additional 10 min. Conversion was determined by reverse phase HPLC analysis on a Supleco Discovery

C18 column (250 × 4.6 mm) using a solvent gradient of 20 to 100% B over 40 min (solvent A, 0.1% TFA/H_2O; solvent B, 0.1% TFA/MeCN). Product identity was confirmed by coelution with a N^5-hydroxy-L-ornithine (L-**3)** synthetic standard Fmoc-derivatized in the same manner and by ESI-HRMS. No product formation was observed in control incubations without NADPH or with enzyme inactivated by boiling.

Kinetic Investigations of VbsO

VbsO *N*-hydroxylase activity was measured at 25 °C in a 300 μL reaction volume containing Tris-HCl (50 mM, pH 8.0), L-ornithine (0.065–5 mM), FAD (50 μM), and NADPH (300 μM). Assays were initiated by the addition of VbsO (250 nM). Activity was monitored continuously on a Cary 50 Bio UV-visible spectrophotometer by following the decrease in absorbance at 340 nm resulting from the conversion of NADPH to $NADP^+$. Initial velocities were calculated from the measured absorbance change over a 0.5–2 min time frame using the extinction coefficient 6,300 $M^{-1}cm^{-1}$. Reactions were run in triplicate and the initial velocity data were fitted to the Michaelis-Menten equation in Kaliedagraph (Synergy Software) to obtain estimates for k_{cat} and K_m.

Assays for VbsA Acyltransferase Activity

To a solution of N^5-hydroxy-L- or D-ornithine **3** (1.2 mM), ((*R*)-3-hydroxybutyryl)-CoA **11** (1 mM), and pH 7.5 Tris buffer (50 mM) at 25 °C was added VbsA (1 μM) to initiate the reaction (total reaction volume of 50 uL). After 8 min the reactions were stopped with 10% TFA (50 μL), chilled at −20 °C for 10 min and centrifuged at 13,000 rpm for 5 min. Conversion was determined by reverse phase HPLC analysis on a Supleco Discovery C18 column (250 × 4.6 mm) using a solvent gradient of 2 to 66% B over 20 min (solvent A, 0.1% TFA/H_2O; solvent B, 0.1% TFA/MeCN). The elution profile was monitored at 220 nm. Product identity was confirmed by coelution with N^5-hydroxy-N^5-((*R*)-3-hydroxybutyryl)-L- or D-ornithine **9** synthetic standards and by ESI-HRMS. No product formation was observed in control incubations omitting VbsA or with enzyme inactivated by boiling.

Kinetic Investigations of VbsA

VbsA acyltransferase activity was measured at 25 °C in a 300 μL reaction volume containing Tris-HCl (50 mM, pH 7.4), N^5-hydroxy-D-ornithine (D-**3**, 0–3 mM) or N^5-hydroxy-L-ornithine (L-**3**, 0–1 mM), 5,5′-dithio-bis(2-nitro-benzoic acid) (DTNB) (50 μM), and ((*R*)-3-hydroxybutyryl)-CoA **11** (300 μM). Assays were initiated by the addition of VbsA (17 nM). Activity was monitored continuously on a Cary 50 Bio UV-visible spectrophotometer by following the increase in absorbance at 412 nm resulting from the reaction between the free thiol of CoASH, generated by VbsA-catalyzed acyl transfer, and DTNB. Initial velocities were calculated from the measured absorbance change over a 0.5–2 min time frame using the extinction coefficient 13,600 $M^{-1}cm^{-1}$. Reactions were run in triplicate and the initial velocity data were fitted to the Michaelis-Menten equation in Kaleidagraph (Synergy Software) to obtain estimates for k_{cat} and K_m.

Assay for VbsL Epimerase Activity

To a solution of N^5-hydroxy-N^5-((*R*)-3-hydroxybutyryl)-D- or L-ornithine **9** (1 mM), PLP (50 μM), and pH 7.75 HEPES buffer (50 mM) was added VbsL (500 nM) to initiate the reaction (total reaction volume of 100 μL). Reaction aliquots (25 μL) were quenched at t = 0, 16, 32, and 64 min with MeCN (50 μL), chilled at −20 °C for 10 min and centrifuged at 13,000 rpm for 5 min. The supernatant was withdrawn and combined with 25 μL of 200 mM borate (pH 8.0). Twenty-five microliters of 10 mM 9-fluorenylmethyl chloroformate (Fmoc-Cl) was added and the reaction was allowed to proceed at room temperature for 5 min. To remove any remaining derivatizing reagent, 25 μL of 0.1 M 1-aminoadamantane was added and the mixture

was kept at room temperature for an additional 30 min. Racemization was determined by reverse phase HPLC analysis on a chiralcel OD-RH column using a solvent gradient of 80 to 100% B over 6 min followed by 100% B for 10 min (solvent A, 0.1% TFA/H_2O; solvent B, 0.1% TFA/MeCN). The elution profile was monitored at 263 nm. Product identity was confirmed by coelution with a similarly Fmoc-derivatized N^5-hydroxy-N^5-((*R*)-3-hydroxybutyryl)-D- or L-ornithine standard **9**. No racemization was observed in control incubations omitting PLP or with enzyme inactivated by boiling.

VbsL Deuterium Incorporation Experiments

A solution of N^5-hydroxy-N^5-((*R*)-3-hydroxybutyryl)-L-ornithine **9** (4 mM) and PLP (50 μM) in pH 7.75 HEPES buffer (50 mM) was prepared (total reaction volume of 1 mL), flash frozen in liquid N_2, and lyophilized for 36 h. The resulting residue was taken up in 950 μL D_2O and incubated with VbsL (2 μM) at room temperature for 18 h. The reaction was halted with 2 mL of MeCN, stored at −20 °C for 20 min and centrifuged at 13,000 rpm for 5 min. The supernatant was withdrawn and combined with 1 mL of 200 mM borate (pH 8.0). Two hundred microliters of 10 mM 9-fluorenylmethyl chloroformate (Fmoc-Cl) was added and the reaction was allowed to proceed at room temperature for 5 min. To remove any remaining derivatizing reagent, 200 μL of 0.1 M 1-aminoadamantane was added and the mixture was kept at room temperature for an additional 30 min. Racemization was determined by reverse phase HPLC analysis on a chiralcel OD-RH column using a solvent gradient of 80 to 100% B over 6 min followed by 100% B for 10 min (solvent A, 0.1% TFA/H_2O; solvent B, 0.1% TFA/MeCN). The elution profile was monitored at 263 nm. Product peaks were collected, flash frozen in liquid N_2, lyophilized overnight, resuspended in MeOH, and analyzed by ESI-HRMS analysis.

ATP-PPi exchange assay to determine activity of the VbsS A domain

A typical experiment (700 μL total volume) was carried as follows: $MgCl_2$ (4 mM), TCEP (5 mM), ATP (5 mM), tetrasodium[^{32}P]pyrophosphate (1 mM, 1.2 μCi), and substrate amino acid (5 mM) were combined in reaction buffer (75 mM Tris, pH 7.5); reactions were then initiated by the addition of VbsGS to a final concentration of 2.0 μM. At regular time intervals, 100 μL aliquots (90 μL for T = 0, before addition of enzyme) were quenched with a 500 μL solution of activated charcoal (1.6% w/v), 200 mM tetrasodium pyrophosphate, and 3.5% perchloric acid in water. The charcoal was pelleted by centrifugation and washed twice with a 500 μL solution of 200 mM tetrasodium pyrophosphate and 3.5% perchloric acid in water. The radioactivity of ATP bound to the charcoal was then measured by liquid scintillation counting. Turnover was calculated as (% incorporation of ^{32}P-PPi)[total PPi]/[Enz].

Isolation of ferrivicibactin

Cell mass from a 50 mL culture of *R. etli* CFN42 (OD_{600} 2.0) grown in MSM minimal media (prepared according to a procedure reported by Dilworth[27]) was suspended in 50 mL fresh media and used to inoculate 500 mL MSM minimal media. The resulting culture was grown at 30 °C for 40 h to an OD_{600} of 1.8. The presence of vicibactin in the culture supernatant during growth was monitored periodically by the Csáky method as described in a report by Dilworth.[19] The culture supernatant was separated from cell debris and harvested by centrifugation and subsequent filtration through a 45 uM filter. According to the Csáky method, [19] the concentration of vicibactin in the filtrate was estimated to be 76 uM. To generate ferric vicibactin for ease of isolation, 496 μL of $Fe(NH_4)_2(SO_4)_2 \cdot 6H_2O$ (0.1 M in H_20) was added and the resulting solution was stirred for 12 h at ambient temperature at which time it took on an orange/red color. The extraction of ferric vicibactin in benzyl alcohol was then carried out as reported previously.[28] The resulting crude methanolic extract containing vicibactin was dissolved in 10 mL H_2O and purified in three portions by preparative HPLC (Phenomenex Luna C_{18}, 250 × 21.2 mm, 10 micron, 100 A column, gradient 0 to 100 % B (B = MeOH with

0.1% TFA v/v, A = H_20 with 0.1 % TFA v/v). The elution of ferric vicibactin at 19 min was detected by UV absorbance at 435 nm. The combined vicibactin containing fractions were concentrated and lyophilized to 8 mg of a red powder.

Isolation of L- and D-desacetylvicibactin

Culture supernatants of J369 and J372,[11] *vbsC* and *vbsL* mutants, respectively, were prepared as reported above for WT *R. etli* CFN42 (growth in MSM minimal media). Siderophore concentration was determined by the Csáky method as for the detection of vicibactin. 250 mL of filtered culture supernatant was concentrated in vacuo to a white solid residue, from which desacetylvicibactin was extracted with 40 mL of MeOH according to a modified literature procedure.[29] The resulting suspension was filtered through a sintered glass frit and again concentrated in vacuo. The extraction procedure was then repeated a second time. Finally, the resulting residue was dissolved in 20 mL 1:1 H_2O:MeOH and purified by preparative HPLC in four portions (Phenomenex Luna C_{18}, 250 × 21.2 mm, 10 micron, 100 A column, gradient 0 to 100 % B (B = MeOH with 0.1% TFA v/v, A = H_20 with 0.1 % TFA v/v). Desferri-deacylvicibactin elutes at 17.3 min with UV detection (220 nm). The combined desacetylvicibactin fractions were concentrated and lyophilized to give 16 mg of L-desacetylvicibactin from J372. Similar yields were obtained for D-desacetylvicibactin from J369. The ^{1}H NMR spectrum of isolated material was analogous to that reported previously.[18]

Assays for VbsC Acetyltransferase Activity

To a solution of desacetyl-D-vicibactin (D-**14**) (1 mM), acetyl-CoA (4 mM), and pH 7.75 HEPES buffer (50 mM) was added VbsC (10 μM) to initiate the reaction (total reaction volume of 350 uL). Reaction aliquots (50 μL) were quenched at t = 0, 1, 2, 4, 8, 16 and 32 min with 10% TFA or 10 mM $Fe(ClO)_3$ in 0.2 M perchloric acid (50 μL). Reactions halted with TFA were chilled at −20 °C for 10 min and centrifuged at 13,000 rpm for 5 min. Reactions halted with $Fe(ClO)_3$ were incubated at ambient temperature for 18 hr and centrifuged at 13,000 rpm for 5 min. Conversion was determined by reverse phase HPLC analysis on a Supleco Discovery C18 column (250 × 4.6 mm) using a solvent gradient of 2 to 66% B over 20 min (solvent A, 0.1% TFA/H_2O; solvent B, 0.1% TFA/MeCN). The elution profile was monitored at 220 nm for the desferri-products and at 435 nm for the ferri-products. Product peaks were collected, flash frozen in liquid N_2, lyophilized overnight, resuspended in MeOH, and analyzed by ESI-HRMS analysis.

Results

Expression and purification of VbsA, VbsC, VbsO, and VbsL

The *vbsA*, *vbsC*, *vbsO* and *vbsL* genes were individually amplified from genomic DNA isolated from *R. etli* CFN42 by PCR and cloned into *E. coli* expression vectors as N- or C-terminal His_6 fusions. The proteins were overexpressed in *E. coli* BL21(DE3) cells at 15 °C with 0.1 mM IPTG and purified using Ni-NTA column chromatography and gel filtration in tandem. VbsA (37.9 kDa, 329 aa) yielded 2.9 mg/L, VbsC (18.5 kDa, 164 aa) yielded 12.0 mg/L, VbsO (50.6 kDa, 453 aa) yielded 0.6 mg/L, and VbsL (43.5 kDA, 396 aa) yielded 0.5 mg/L. All proteins were purified to near homogeneity with a correct molecular weight as judged by SDS-PAGE (Figure S1). The flavin dependent monooxygenase VbsO purified with FAD as bound cofactor, as determined by analytical HPLC using authentic standards (data not shown). However, using UV-vis spectroscopy, the FAD occupancy was determined to be less than 5%.

Expression and purification of VbsS and VbsG

The *vbsGS* transcript was amplified from *R. etli* CFN42 genomic DNA and cloned into a pET24b *E. coli* expression vector to append a C-terminal His_6 tag to *vbsS* (*vbsG* untagged). The proteins were overexpressed in *E. coli* BL21(DE3) cells at 15 °C following induction with IPTG, and purified by $(NH_4)_2SO_4$ precipitation and gel filtration in tandem. SDS-PAGE analysis of the eluted fractions and in gel tryptic digest and MS sequencing (Figure S2) indicated that VbsG (8 kDa) co-purifies with the 147 kDa VbsS. Although the VbsGS expression construct incorporates a C-terminal His_6 tag, we found that VbsS does not bind to Ni for affinity purification. VbsS alone, either N or C-His tagged exhibits similar behavior; however, in an initial screen, the VbsGS expression vector was produced in the highest yield following $(NH_4)_2SO_4$ precipitation; therefore the two co-purified proteins VbsGS were utilized for activity assays.

Synthesis of N^5-hydroxy-D- and L-ornithine (D- and L-3) and N^5-((*R*)-3-hydroxybutyryl)-N^5-hydroxy-D- and L-ornithine (D- and L-9)

The requisite hydroxylamine substrates were prepared using an indirect oxidation method developed by Miller and coworkers[30] (Scheme 1). Starting with commercially available N^2-Boc-D- or L-ornithine (**1**), the primary amine was converted to an imine followed by the mCPBA oxidation to the oxaziridine. Treatment with TFA isomerized the oxaziridine to a nitrone and afforded amino acids D- and L-**2** in 45% and 42% respectively over three steps. Finally, acid catalyzed hydrolysis of the nitrone afforded the HCl salts of D-**3** in 35 % yield and L-**3** in 78% yield.

The hydroxamate substrates D- and L-**9** were prepared using a synthetic scheme based on methodology first illustrated by Milewska and Chimiak[31] and later optimized by Phanstiel.[32] As shown in Scheme 2, oxidation of the free amine of N^2-Boc-D- or L-ornithine *tert*-butyl ester (**4**) with benzoyl peroxide afforded the corresponding N^5-(benzoyloxy)amines D-**5** and L-**5** in 36% and 80% yield respectively. Subsequent acylation with acid chloride **6** under biphasic conditions afforded the fully protected hydroxamates D- and L-**7** in 97% yield for both compounds. Subsequent removal of the benzoyl (Bz) and acetyl (Ac) protecting groups by treatment with a 10% NH_3/MeOH solution and of the *tert*-butyl-carbonate (Boc) and *tert*-butyl (*t*-Bu) groups with trifluoroacetic acid (TFA) provided the TFA salts of D-**9** in 51% overall yield from D-**7** and L-**9** in quantitative yield from L-**7**.

Detailed synthetic protocols and spectroscopic data can be found in the Supporting Information.

Characterization of VbsO

The product of the *vbsO* gene is homologous to IucD,[33] CchB[34] and PvdA,[35] flavin-dependent monooxygenases[36] from *E. coli*, *S. coelicolor* and *P. aeruginosa* respectively. IucD catalyzes the regiospecific hydroxylation of the ε-amino group of L-lysine as the first step in biosynthesis of the hydroxamate containing siderophore aerobactin, while CchB and PvdA carry out hydroxylation of the δ-amino group of L-ornithine as the first committed step in coelichelin and pyoverdine biosynthesis respectively. Therefore, we anticipated that VbsO-mediated N^5-hydroxylation of ornithine would be the starting point in the biosynthesis of vicibactin as well.

To evaluate the catalytic activity of VbsO, the recombinant enzyme was incubated with L-Orn in the presence of FAD and NADPH. To facilitate identification and detection of the hydroxylated amino acid, the assays were derivatized with 9-fluorenylmethyl chloroformate (Fmoc-Cl) to yield highly UV active Fmoc derivatives. As shown in figure 3, the enzymatic incubation with L-Orn and subsequent derivatization with Fmoc-Cl resulted in the formation of a new peak in the analytical HPLC trace with a retention time consistent with authentic

N^5-hydroxy-L-Orn bisFmoc standard, bisFmoc-L-**3**. Further confirmation of product formation was obtained by ESI-HRMS analysis ([M+Na]+ *m*/*z* calcd., 615.2107; found, 615.2114) of the new species purified by HPLC (Figure S3). No activity was detected with enzyme inactivated by boiling or in the absence of NADPH (data not shown).

The Michaelis-Menten kinetic parameters of VbsO for L-Orn hydroxylation were determined to an apparent k_{cat} of 108 ± 2 min^{-1} and K_M of 0.305 ± 0.024 mM, as determined by monitoring the conversion of NADPH to $NADP^+$ at 340 nm (Figure 3C). For comparison, the apparent K_M value of VbsO for L-Orn is similar to the reported K_M values of PvdA[35] for L-Orn (0.593 mM) and IucD[33] for L-Lys (0.11 mM) and tenfold lower than the reported K_M value of CchB[34] for L-Orn (3.6 mM). Regarding the catalytic efficiencies (k_{cat}/K_m) of the three L-ornithine N^5-hydroxylases, VbsO shows a tenfold higher efficiency (354.10 $min^{-1}mM^{-1}$) than PvdA (44.52 $min^{-1}mM^{-1}$) and a hundredfold higher efficiency that CchB (4.83 $min^{-1}mM^{-1}$).

To probe the substrate specificity of the enzyme, we tested D-Orn, L- or D-Lys, and N^5-((*R*)-3-hydroxybutyryl)-L- or D-Orn (L- or D-**10**) for VbsO-mediated hydroxylation by spectrophotometric measurement of NADPH oxidation and HPLC product analysis. When D-Orn was employed as a substrate, no NADPH oxidation or hydroxylated product formation was observed, indicating that VbsO is specific for the L isomer of Orn (Figure 3B). Both D- and L-lysine were found to be non-substrate effectors of VbsO, as they activated NADPH oxidation, however no N^6-hydroxylysine was detected by analytical HPLC (Figure S4). Finally, N^5-((*R*)-3-hydroxybutyryl)-L- and D-Orn (**10**) were tested to probe the timing of hydroxylation in the vicibactin biosynthetic pathway as well as VbsO substrate specificity. Neither compound was found to be a substrate nor a non-substrate effector of VbsO as no hydroxylated product or NADPH oxidation was observed (Figure S5).

Characterization of VbsA

The VbsA protein exhibits sequence similarity to several bacterial acyltransferases[11] found in gene clusters associated with the biosynthesis of hydroxamate containing siderophores. The most notable homolog is IucB,[37] a biochemically characterized acetyl-CoA-dependent N^6-hydroxylysine N^6-acetyltransferase involved in the biosynthesis of the *E. coli* siderophore aerobactin. We hypothesized that VbsA catalyzes the transfer of an (*R*)-3-hydroxybutyryl group from the CoA thioester **11** to N^5-hydroxy-ornthine **3** to form N^5-((*R*)-3-hydroxybutyryl)-N^5-ornithine **9** (Figure 4). Although genes encoding for the enzymes necessary for the biosynthesis of thioester **11** are not found in the Vbs cluster, *Rhizobium* species are known to utilize **11** for the production of polyhydroxybutyrate[38] thereby indicating its bioavailability in the cell.

Initial activity assays revealed that incubation of VbsA with synthetic L-**3** and thioester **11** resulted in the formation of two new peaks in the analytical HPLC trace with retention times of 6.6 min and 8.5 min, identical to that of hydroxamate L-**9** and CoASH respectively, which were absent from control experiments in which VbsA was omitted (Figure 4B). The compound eluting at 6.6 min was isolated and subjected to MS to confirm its identification as hydroxamate L-**9**. ESI-HRMS analysis confirmed the presence of a compound with the molecular formula $C_9H_{18}Na_1N_2O_5^+$ (calc.: 257.1108, found: 257.1109), consistent with the sodium adduct ion of **9** (Figure S6).

At the outset of these studies the timing of C^2-epimerization of the ornithine moiety in the vicibactin scaffold was not known. We therefore questioned if VbsA would also recognize D-**3** as the hydroxylamine acceptor. Initial activity assays indicated that D-**3** is also a viable substrate for VbsA and yielded two new peaks in the analytical HPLC trace with retention times of 6.8 and 8.5 min, identical to that of D-**9** and CoASH respectively, which were absent

from control experiments in which VbsA was omitted (Figure 4B). ESI-HRMS analysis of the peak at 6.8 min further confirmed the product identity as D-**9** ($[M + Na]^+$, *m*/*z* calc.: 257.1108, found: 257.1112) (Figure S7).

To gain further insight into the substrate specificity of VbsA, kinetic studies were undertaken with hydroxylamines L- and D-**3** by monitoring the rate of CoASH formation using the DTNB assay. At a fixed thioester **11** concentration of 300 μM, the K_m of VbsA for L-**3** was 17.9 ± 2.1 μM and the k_{cat} for the reaction was 504 ± 12 min^{-1} (Figure 4C). Under the same assay conditions, the K_m of VbsA for D-**3** was 319 ± 47 μM, and the k_{cat} was 1960 ± 98 min^{-1}. Using the catalytic efficiency criterion (k_{cat}/K_m), L-**3** is only a 5-fold better substrate than the D-isomer.

The hydroxylamine promiscuity of VbsA is analogous to that of IucB, which was shown to fully acetylate both enantiomers of N^6-hydroxylysine as well as N^5-hydroxy-L-ornthine **3**, *N*-methylhydroxylamine and even hydroxylamine. However, Neiland and coworkers found that IucB[39] is selective for hydroxylamines over amines, as Lys was not a substrate. To test if VbsA would recognize amine substrates as acyl acceptors, VbsA was incubated with D- or L-Orn and thioester **11** and the formation of CoASH using the DTNB assay was monitored (Figure S8). At pH 8.0 with 1 mM substrate, increase in the absorbance at 412 nm was not observed, which shows acyl transfer is not occurring and confirms that D- and L-Orn are not efficient substrates for VbsA.

Having established that VbsA is selective for hydroxylamines over amines, we investigated whether the enzyme is capable of transferring acyl groups from CoA substrates other than **11** to hydroxyamine L-**3**. Preliminary activity assays revealed that incubation of VbsA and hydroxylamine L-**3** with ((*S*)-3-hydroxybutyryl)-CoA (**12**), butyryl-CoA (**13)** and even acetyl-CoA resulted in the formation of two new peaks in the analytical HPLC trace with retention times and masses consistent with the expected hydroxamate product and CoASH (Figure S9). The acyl-CoA promiscuity of VbsA is in contrast to the high selectivity IucB shows for its cognate acyl-CoA substrate, acetyl-CoA. Neiland and coworkers reported that in activity assays with IucB, propionyl CoA was no more than 5% as active as acetyl-CoA and isobutyryl-CoA was not utilized as a substrate.

Characterization of VbsL

One of the notable features of vicibactin is that the ornithine residue embedded in its scaffold is in the D-configuration.[40] Inspection of the VbsS NRPS module does not reveal an epimerization domain (see below). Instead, Carter et al.[11] proposed that VbsL, predicted to be a PLP-dependent enzyme,[41] is responsible for the C^2 L- to D-configuration change in the Orn scaffold. PLP-dependent enzymes that have racemase/epimerase activity normally work on free amino acids rather than aminoacyl thioesters; therefore, we expected that VbsL would work before VbsS in the vicibactin biosynthetic pathway. However, the substrate promiscuity of VbsA, shown to acylate both enantiomers of hydroxylamine **3** (see above), could allow epimerization to occur before or after hydroxamate formation. Therefore, our initial assays focused on ascertaining whether N^5-hydroxyornithine **3** or N^5-((*R*)-3-hydroxybutyryl)-N^5-hydroxyornithine **9** are substrates for VbsL.

Initial activity assays indicated that hydroxylamine **3** is not an efficient substrate for VbsL. Incubation of VbsL (10 μM) with L- or D-**3** and PLP followed by Fmoc-derivatization and analysis by chiral HPLC (Chiralcel OD-RH) and comparison to similarly Fmoc-derivatized synthetic standards showed only a trace amount of epimerization of the amino acids had occurred after 2 hr (Figure S10). In contrast, incubation of hydroxamate L-**9** with VbsL (0.5 μM) and PLP followed by Fmoc-derivatization and analysis by chiral HPLC showed complete racemization had occurred after 1 hr (Figure 5B). Racemization was also observed when

D-**9** was incubated with VbsL under the same conditions, confirming that both diastereomers are accepted as substrates for VbsL (Figure 5C). No racemization activity was detected with enzyme inactivated by boiling or in the absence of PLP (data not shown).

A general mechanism for enzymatic PLP-dependent epimerization/racemization involves the formation of a Schiff-base between the C^2-amino group and PLP. This intermediate facilitates the deprotonation and reprotonation at the α-position by conserved residues in the enzyme, resulting in epimerization/racemization of the substrate. Therefore, assays of VbsL performed in D_2O should result in enzyme-dependent incorporation of deuterium into the substrate. VbsL was incubated with L-**9** and PLP in D_2O for 18 hr followed by Fmoc-derivatization. The resulting bisFmoc diastereomers were separated using chiral HPLC and the product peaks were collected. The molecular formula of the compound that coeluted with bisFmoc-L-**9** was found to be $C_{39}H_{37}DN_2NaO_9^+$ (calc.: 702.2532, found: 702.2539), as was that of the compound that coeluted with bisFmoc-D-**9** (calc.: 702.2532, found: 702.2518) by LC-QTOF-HRMS analysis, consistent with deuterium incorporation into **9**.

Characterization of VbsS

Translated *vbsS* has 1331 amino acid residues and contains four discernable domains by sequence analysis. The N-terminal domain displays significant sequence similarity to a condensation (C) domain and contains all seven signature sequences (C1-C7). The catalytic core of C domains has the consensus sequence HHXXXD,[42,43] in which the second histidine and the terminal aspartic acid residues have been shown to be critical for catalytic activity. In VbsS, however, the critical histidine is replaced with a proline. This mutation suggests that the C domain is not catalytically active and does not serve a role in the biosynthesis of vicibactin.

The condensation domain in VbsS is followed by an adenylation (A) domain; such domains are bifunctional catalysts for both aminoacyl-AMP formation and subsequent loading of the activated amino acid onto the free thiol of the Ppant group on the cognate thiolation (T) domain. The specificities of A domains in NRPS modules can be predicted using an NRPS code in which the identity of eight amino acids in the A domain between a conserved aspartate and lysine confer specificity.[44,45] However, a careful comparison of the VbsS A domain amino acid code (DGESSGGMTK) to those in the data bank did not find any significant homology to A domains of known specificity, and showed that it is significantly different from A domains known to activate Orn or N^5-hydroxyornithine[46] (Table S1). To determine the substrate specificity of the VbsS A domain, the classical ATP-pyrophosphate (PPi) exchange assay was used to monitor the reversible incorporation of [^{32}P]PPi into ATP in a substrate-dependent fashion[47] (Figure 6). In the presence of 5 mM amino acid, the relative activities were obtained as follows: D-**9** (100%), L-**9** (28.6%), L-**3** (0.9%), D-**3** (0.04%), L-Orn (0.7%), and D-Orn (0.04%) (Figure 6). This data clearly shows that hydroxamate D-**9** is the preferred substrate for VbsS; however, the C^2-L diastereomer (L-**9**) is also recognized to a lesser extent. Interestingly, we find that C-His_6-tagged VbsS, expressed without VbsG, is not active in the ATP-PPi exchange assay. The role of VbsG in VbsS activity is not yet clear and is the subject of ongoing investigation.

Protein sequence alignment indicated that the third domain in VbsS resembles a typical carrier protein or T domain in NRPS systems with Ser^{1010} as the proposed site for posttranslational priming with phosphopantetheine to convert inactive apo T domains into active holo domains. The purified VbsSG complex was assayed for covalent attachment of a phosphopantetheinyl group by Sfp, a phosphopantetheinyltransferase from *B. subtilis* with broad specificity. Under the assay conditions, Sfp rapidly (15 min) modified VbsS with [^{14}C]Ac-CoA as a test substrate for acyl-pantetheinylation. The stoichiometry of Ppant incorporation was estimated to be ~50% based on the specific radioactivity of [^{14}C]Ac-CoA and the concentration of VbsS in the VbsSG pair (Data not shown).

Although there is a C-terminal thioesterase domain in VbsS which should be the cyclotrimerization catalyst for D-**9** chains bound to the T domain our assays so far with either VbsS or the VbsSG complex did not detect release of desacetylvicibactin (D-**14**). Detailed assessment of whether VbsS accumulates tethered linear dimeric and trimeric forms of D-**14** on the T domain and/or the TE domain prior to cyclization to the 30 membered tri-lactone scaffold in analogy to the action of enterobactin synthetase will be the subject of a subsequent study.

Characterization of VbsC

The final step in vicibactin biosynthesis is proposed to be N^2-acetylation of the three ornithine residues in desacetylvicibactin. Based on genetic knockout studies and bioinformatic analysis, Carter et. al. predicted that VbsC is the acetyltransferase in the Vbs cluster.[11] A knockout of *vbsC* was studied in transconjugants of *Paracoccus denitrificans* and led to the generation of a functional siderophore as judged by the chrome azurol S assay[48] (CAS). However, MS analysis of the supernatant from a culture of *P. denitrificans* harboring the *vbsC* mutant did not reveal a peak corresponding to vicibactin but instead had a peak of 649.7, corresponding to desacetylvicibactin (**14**). Interestingly, *vbsL* knockout strains also produced **14**, suggesting that VbsC is specific for the C^2-D-configuration in the ornithine moiety.

In order to investigate the activity and selectivity of VbsC, we first obtained the C^2-D- and L-isomers of desacetylvicibactin **14** from *L. leguminosarum* strains with either *vbsC* or *vbsL* inactivated[11] (generously provided by Prof A.W.G. Johnston). After growing the strains under iron-deficient conditions, we used preparative HPLC to separate out and purify the desacetylvicibactin isomers from the supernatant. Desacetylvicibactin **14** has a distinct UV profile with an absorbance maximum at 210 nm that aided in the detection of this siderophore. The identity of the previously characterized apo-siderophores was confirmed by HRMS and ^{1}H NMR analysis (Figure S11 and S12); stereochemistry was determined by saponification of the tri-ester with LiOH, and chiral HPLC analysis of the resulting monomer in comparison with diastereomeric standards prepared synthetically (Figure S13).

With the C^2-D- and L-isomers of desacetylvicibactin in hand we first incubated purified VbsC with D-**14** and acetyl-CoA for 1, 2, 4, 8, 16 and 32 min. The reactions were halted by the addition of TFA and HPLC analysis revealed the time dependent appearance of three new peaks in the analytical HPLC chromatogram with retention times of 11.0, 11.9 and 12.8 min, which were absent from control reactions containing VbsC inactivated by boiling (Figure 7). The compounds with retention times of 11.0 and 11.9 min were isolated from a large-scale incubation that was stopped after 8 min. The molecular formula for the peak at 11.0 min was deduced to be $C_{29}H_{51}N_6O_{13}^+$ (calc.: 691.3509, found: 691.3535) by ESI-HRMS analysis, consistent with the protonated ion of monoacetyled **15** (Figure S14). ESI-HRMS analysis of the peak at 11.9 min yielded a molecular formula of $C_{31}H_{53}N_6O_{14}^+$ (calc.: 733.3614, found 733.3622) consistent with the protonated ion of diacetylated **16** (Figure S15). The compound with a retention time of 12.8 min was isolated from a large-scale reaction that was stopped after 32 minutes and ESI-HRMS analysis yielded the molecular formula $C_{33}H_{55}N_6O_{16}^+$ (calc.: 775.3777, found 775.3735) confirming its identity as protonated vicibactin (**VB**, Figure S16).

To further verify that VbsC is indeed catalyzing conversion of desacetyl-D-vicibactin **14** to vicibactin, an assay containing VbsC, D-**14** and acetyl-CoA was halted after 1 hr by the addition of $Fe(ClO)_3$, which precipitated the enzyme and converted the product to its corresponding ferric complex. A new peak in the HPLC trace that coeluted with authentic ferrivicibactin (isolated from wild type *R. etli*) and exhibited tri-hydroxamate-Fe complex absorption (λ max = 435 nm) was observed and ESI-MS analysis indicated a mass consistent with ferri-vicibactin ($[M + H]^+$ *m*/*z* calcd.: 828.2835, found: 828.2855) (Figure S17 and S18).

As noted above, VbsC is proposed to be specific for desacetylvicibactins bearing a C^2-D-configured ornithine moiety owing to the isolation of desacetylvicibactin from VbsL (**9**-epimerase) mutants grown in iron-deficient media. To test this hypothesis, VbsC was incubated with L-**14** and acetyl-CoA under the same conditions as for D-**14** and the formation of CoASH was monitored by UV using the DTNB assay. No increase in the absorbance at 412 nm (due to the reaction between the free thiol of CoASH, generated by enzyme-catalyzed acyltransfer, and DTNB was observed), highlighting the strong preference of VbsC for D-**14** (Figure S19). Furthermore, analytical HPLC analysis of reactions halted after 2 hr by the addition of either TFA or $Fe(ClO)_3$[19] indicated that negligible acetylation of L-**14** had occurred (data not shown).

Discussion

Nature seems to have specifically formulated the hydroxamic acid functionality[49] to serve as a site of iron ligation in siderophore scaffolds. As such, the majority of hydroxamate-containing natural products are associated with some aspect of iron transport. Hydroxamates have the ability to capture ferric iron through a stable five membered ring chelate and when arranged in a trimer, as in the siderophore vicibactin, a tight six coordinate species results (see Figure 1). Tri-hydroxamates comprise the primary siderophores essential to the growth of a variety of microorganisms ranging from pathogens to beneficial agriculture symbionts. Included are the 33-membered desferrixoamines[13] from *Streptomycetes*, the 36-membered fusarinine C^{10} of *Aspergillus* fungal strains, and the 30-membered vicibactin from *Rhizobia*. Each of these macrocycles is the result of an enzymatic cyclotrimerization of 11, 12, and 10-atom monomer units, respectively. During the oligomerization-cyclization reactions involved in the biosynthesis of the cyclic triesters, a terminal hydroxyl group acts as a nucleophile to capture a NRPS-bound activated acyl thioester of a separate monomer for two head to tail esterifications; macrocyclization occurs by intramolecular capture of a TE domain-bound ester. The NRPS-thiotemplated cyclotrimerization differs from stand-alone macrocyclization catalysts (NRPS-independent) that catalyze ATP-dependent condensation reactions between soluble intermediates, shown to be operative for amide bond formation and yielding triamide hydroxamates such as desferrioxamine E. Current data suggests the NIS pathway[14] may have evolved for triamides, while NRPSs are utilized to generate triester siderophores.

As part of an effort to understand the origin and role of *N*-hydroxylation in the transformation of readily available amino acids into non-ribosomal peptides and related small molecules, we have investigated the bacterial strategy for tri-hydroxamate biosynthesis in the context of vicibactin. Through *in vitro* characterization of recombinant vicibactin biosynthetic proteins and comparison of the enzymatic products with authentic synthetic standards, we have been able to elucidate the timing and logic of the hydroxamate monomer synthesis. In *Rhizobia*, vicibactin is assembled in the cytoplasm, exported into the rhizosphere, and then re-imported as the Fe-chelate. The ferric-bound complex provides the Fe essential to the assembly of active endogenous nitrogenases; these enzymes are involved in maintaining a usable source of nitrogen for symbiotic host legumes. Microbial siderophores have also been linked to iron availability in plants; these factors suggest that siderophore biosynthesis in *Rhizobia* is a critical component of productive symbiosis.

Genes for the biosynthesis of vicibactin were identified by Carter and coworkers in 2002, and reveal the presence of a key non-ribosomal peptide synthetase, VbsS, presumably responsible for assembly of the trimer, and several tailoring enzymes that convert L-Orn to the functionalized hydroxamate monomer **9**. Genetic studies indicate that, in addition to *vbsS*, *vbsA*, *G*, and *O*, encoding an acyltransferase, an MbtH-like protein,[50] and an *N*-hydroxylase, respectively, are essential for vicibactin production. In contrast, insertional mutants of *vbsC* (encoding an acyltransferase) and *vbsL* (an epimerase) produce desacetylated form(s) of vicibactin. Bioinformatic analysis suggests that the 10-atom monomer chain is derived from

L-Orn, but does not reveal the sequence of modification events. Although tailoring of L-Orn could occur in trans while the substrate is tethered to the T domain of VbsS, as suggested by Carter, an alternative pathway, detailed here, involves complete elaboration of the desacetyl-hydroxamate monomer before utilization by the VbsS adenylation domain.

Previous studies of siderophore biosynthesis support our findings that VbsS activates functionalized Orn. For example, early investigation of the fusigen synthetase, analyzed in cell free extracts, indicated the direct utilization of a fully functionalized hydroxamate monomer.[51] A key differentiating feature of fungal and bacterial hydroxamate siderophores is the configuration of the Orn residue (D vs L). It has not been determined why this difference is maintained, but one objective of our study was to determine the gate-keeping mechanism that shuttles only the D-isomer through the vicibactin assembly line.

We began our investigation with VbsO, a flavin-dependent hydroxylase able to generate reduced flavin with NADPH without the need for an external reductase, and found that it is site- and stereo-specific for the distal nitrogen in L-Orn. The intermediate peroxy-flavin species that serves as the active hydroxylation catalyst requires nucleophilic attack for oxygen transfer. This mechanism is supported by the fact that while the N^5-amino group of L-Orn is a substrate for *N*-hydroxylation, the less nucleophilic N^5-acyl-derivative **10** of either D or L-Orn is unreactive.

VbsA is homologous to CoA-dependent *N*-acyl transferases; based on VbsO data, we suspected that VbsA acts on a soluble hydroxylamine, rather that the primary amine. Our results show N^5-hydroxyornithine **3** and not Orn is selectively acylated - a necessary gatekeeping function to ensure that the key hydroxamate functionality required for iron coordination is assembled. The fact that VbsA is promiscuous and accepts both the L and D configuration of hydroxylamine **3** opens the question of when the C^2-position of the Orn residue is epimerized. This issue has been resolved as noted below. In the utilization of thioester **11**, available from primary fatty acid metabolism, VbsA also installs the essential hydroxy group that enables downstream head to tail trimerization of the monomer.

The stereochemistry at the C^2-position in each monomer unit is essential for the formation of a well defined Fe hexadentate chelation, and dictates the chirality of the resulting complex.[52] As fungal siderophores are predominantly of the L-configuration, the use of a D-Orn derivative by *Rhizobia* could be a strategy to protect the metabolic investment in vicibactin biosynthesis by limiting the use of ferri-vicibactin by other microorganisms in the rhizosphere. A general mechanism in secondary metabolism for the formation of D-amino acid residues involves enzyme catalyzed exchange of the α-proton, rendered acidic by either formation of a thioester (a covalently tethered substrate to an NRPS module), or a PLP-derived Schiff base of a soluble substrate. Bioinformatic analysis of the VbsS NRPS module does not reveal an epimerization domain, and therefore suggests that formation of the D-Orn isomer occurs prior to trimerization. *In vitro* studies of VbsL, a PLP-dependent epimerase, corroborates the hypothesis that the preferred substrate is the free hydroxamate **9**. VbsL is highly selective for **9**, and does not efficiently process either L-Orn, or hydroxylamine **3**, despite the availability in each of the requisite free amine for Schiff base formation. The selection of the hydroxamate monomer by VbsL also explains why VbsA does not need to maintain selectivity for the stereochemistry at the C^2-position of the hydroxylamine as only the L-isomer is available for acylation. We have therefore shown that VbsO, A, and L are necessary and sufficient to generate the desacetyl-hydroxamate moiety embedded in the vicibactin trimeric structure.

Along with several tailoring enzymes, the vicibactin gene cluster also encodes the NRP synthetase VbsS. While biochemical characterization of VbsO, A, L has elucidated the origin of the densely functionalized 10 atom monomer, analysis of VbsS would further substantiate

the postulated trimerization mechanism. The 147 kDa VbsS was originally difficult to obtain in purified form through Ni-affinity chromatography of the His_6-tagged construct; however, it was possible to achieve purification by ammonium sulfate fractionization and size exclusion column chromatography of heterologously expressed *vbsGS*. Coexpression of VbsS with the MbtH-like protein[50] VbsG provided increased amounts of the active synthetase in the purified protein fraction for reasons that are not yet understood. Although their function has not yet been elucidated, small 7–8 kDa MbtH-like proteins are cotranscribed in many NRPS-encoding gene clusters and have been shown to be important for metabolite assembly *in vivo*.[50] The role of VbsG in improved solubility, stability, or activity of VbsS is the subject of ongoing investigation.

While the N-terminal C (condensation) domain of VbsS is presumably not functional based on sequence analysis, it was possible to assay the first catalytic step performed by the synthetase A domain. Analysis of the ATP-dependent conversion of the substrate carboxylic acid into the aminoacyl-AMP ester in the presence of VbsS was accomplished by measuring the incorporation of ^{32}PPi in ATP as a result of reversible substrate activation. The use of several candidate Orn-derived monomers in this ATP-PPi exchange experiment indicated the hydroxylamines L- and D-**3** (and L- and D-Orn) are not accepted as substrates, and that, while the D-**9** diastereomer is preferred, the L-**9** diastereomer is activated to a lesser extent. While we have not yet succeeded in reconstitution of the cyclotrimerization *in vitro*, our results indicate that the incomplete selectivity of the VbsS domain for D- vs L-**9** activation is consistent with detection of both D- and L-desacetylvicibactin isomers in mutant strains noted below.

Genetic knockouts in the vicibactin gene cluster, prepared and studied in transconjugants of *Paracoccus denitrificans* by Carter and coworkers,[11] further address the issue of stereoselection in vicibactin biosynthesis and point to the secondary gatekeeping function of the last-acting acyltransferase VbsC. While the *vbsC* mutant makes desacetylvicibactin as expected, the *vbsL* knockout also produces a functional siderophore of the same molecular weight, presumed to be the L-isomer of desacetylvicibactin **14**. These data suggests that VbsL and VbsC each act at different stages of assembly to ensure only the trimer of the D-ornithine containing monomer is elaborated to mature vicibactin. In order to confirm the stereoselectivity conferred by VbsC, we isolated two samples of desacetylvicibactin **14** from the *vbsL* and *vbsC* knockouts and tested each *in vitro* as substrates for purified VbsC. Confirmation of the suggested stereochemistry of the starting material trimers was accomplished by saponification and comparison of the resulting monomer with synthetic D and L-hydroxamate **9** by chiral HPLC. Corroborating the *in vivo* work, purified VbsC only accepts the trimer of the D-hydroxamate **9** for acetyltransfer with acetyl-CoA to produce mature vicibactin, identified following treatment with Fe by coelution with an authentic sample of ferrivicibactin isolated from *R. etli* CFN42 and HRMS. The purification of ferrivicibactin from *R. etli* CFN42 is also noteworthy as it confirms our initial assumption that vicibactin is a native siderophore of this strain.

Hydroxamates are a common motif in bacterial siderophore scaffolds, and a prevalent mechanism for iron capture in fungi. Several strategies have coevolved for hydroxylamine acylation to produce the ubiquitous hydroxamate with distinct acyl moieties. In *Pseudomonas*, an NRPS C domain catalyzes acylation of phosphopantetheinyl-tethered oxazolinyl acyl moiety with soluble *N*-hydroxy-histamine to generate prepseudomonine in the chain release step.[53] For desferrioxamine E production in *Streptomyces coelicolor*, ligation of *N*-hydroxycadaverine with a succinyl group from the Krebs cycle metabolite succinyl-CoA is promoted by an acyltransferase belonging to the GNAT family.[13] Coelichelin biosynthesis in *Streptomyces coelicolor* involves hydroxylamine formylation catalyzed by the formyl transferase CchA in the presence of N^{10}-formyltetrahydrofoloate.[54] In the case of vicibactin, we find the acyltransferase VbsA couples a ((*R*)-3-hydroxybutyryl)-CoA **11** from lipid

metabolism with N^5-hydroxyornithine **3**. While there are a variety of mechanisms for acylation, flavin dependent *N*-hydroxylases are commonly the source of the hydroxyl amine;[36] a majority act on aliphatic (Orn, Lys, histamine, cadaverine), and therefore nucleophilic, amine substrates. Mycobactin biosynthesis is a single example where a flavoenzyme-mediated hydroxylation is suggested to follow amine acylation.[55] On the one hand this order of acylation then hydroxylation would avoid formation of the potentially unstable hydroxylamines; however this sequence requires the amide to be sufficiently nucleophilic for *N*-hydroxylation by the peroxy-flavin intermediate. Given the essential role of flavin-monooxygenases in the biosynthesis of virulence-associated siderophores such as mycobactin[55] from *Mycobacterium tuberculosis* and pyoverdine[56] from *Pseudomonas aeruginosa*, further structural and functional analysis could be of value for the development and identification of new therapeutic targets.[57]

Supplementary Material

Refer to Web version on PubMed Central for supplementary material.

Acknowledgments

This work was supported by an NIH grant to C.T.W (AI042738) and by an NIH NRSA fellowship to J.R.H (F32GM083464); Elizabeth S. Sattely is a Damon Runyon Fellow supported by the Damon Runyon Cancer Research Foundation (DRG-1980-08). We thank Prof. Andrew W. B. Johnston for provision of *R. leguminosarum* strains J372 and J369 and Prof. Dewey G. McCafferty and Amanda Jane Hoertz for helpful suggestions regarding the purification of VbsS.

References

1. Miethke M, Marahiel MA. Microbiol Mol Biol Rev 2007;71:413–51. [PubMed: 17804665]
2. Renshaw JC, Robson GD, Trinci APJ, Wiebe MG, Livens FR, Collison D, Taylor RJ. Mycol Res 2002;106:1123–1142.
3. Barry SM, Challis GL. Curr Opin Chem Biol 2009;13:205–15. [PubMed: 19369113]
4. Crosa JH, Walsh CT. Microbiol Mol Biol Rev 2002;66:223–49. [PubMed: 12040125]
5. Gehring AM, Mori I, Walsh CT. Biochemistry 1998;37:2648–59. [PubMed: 9485415]
6. Miller DA, Luo L, Hillson N, Keating TA, Walsh CT. Chem Biol 2002;9:333–44. [PubMed: 11927258]
7. Patel HM, Tao J, Walsh CT. Biochemistry 2003;42:10514–27. [PubMed: 12950179]
8. Fischbach MA, Walsh CT. Chem Rev 2006;106:3468–96. [PubMed: 16895337]
9. Hissen AH, Wan AN, Warwas ML, Pinto LJ, Moore MM. Infect Immun 2005;73:5493–503. [PubMed: 16113265]
10. Eisendle M, Oberegger H, Zadra I, Haas H. Mol Microbiol 2003;49:359–75. [PubMed: 12828635]
11. Carter RA, Worsley PS, Sawers G, Challis GL, Dilworth MJ, Carson KC, Lawrence JA, Wexler M, Johnston AW, Yeoman KH. Mol Microbiol 2002;44:1153–66. [PubMed: 12028377]
12. Eng-Wilmot DL, Rahman A, Mendenhall JV, Grayson SL, van der Helm D. Journal of the american chemical society 1984;106:1285–1290.
13. Barona-Gomez F, Wong U, Giannakopulos AE, Derrick PJ, Challis GL. J Am Chem Soc 2004;126:16282–3. [PubMed: 15600304]
14. Challis GL. Chembiochem 2005;6:601–11. [PubMed: 15719346]
15. Kadi N, Arbache S, Song L, Oves-Costales D, Challis GL. J Am Chem Soc 2008;130:10458–9. [PubMed: 18630910]
16. Kadi N, Oves-Costales D, Barona-Gomez F, Challis GL. Nat Chem Biol 2007;3:652–6. [PubMed: 17704771]
17. Schrettl M, Bignell E, Kragl C, Sabiha Y, Loss O, Eisendle M, Wallner A, Arst HN Jr, Haynes K, Haas H. PLoS Pathog 2007;3:1195–207. [PubMed: 17845073]
18. Dilworth MJ, Carson KC, Giles RGF, Byrne LT, Glenn AR. Microbiology 1998;144:781–791.

19. Carson KC, Holliday S, Glenn AR, Dilworth MJ. Arch Microbiol 1992;157:264–71. [PubMed: 1387306]
20. Barton, LL.; Johson, GV.; Bishop, YM. Iron Nutrition in Plants and Rhizospheric Microorganisms. Barton, LL.; Abadia, J., editors. Springer; Netherlands: 2006. p. 199-214.
21. Bloemberg GV, Lugtenberg BJ. Curr Opin Plant Biol 2001;4:343–50. [PubMed: 11418345]
22. Stacey, G. The Biological N-Cycle. Bothe, H.; Ferguson, SJ.; Newton, WE., editors. Elsevier; 2007. p. 147-164.
23. Rubio LM, Ludden PW. Annu Rev Microbiol 2008;62:93–111. [PubMed: 18429691]
24. Haas H, Eisendle M, Turgeon BG. Annu Rev Phytopathol 2008;46:149–87. [PubMed: 18680426]
25. Gonzalez V, Santamaria RI, Bustos P, Hernandez-Gonzalez I, Medrano-Soto A, Moreno-Hagelsieb G, Janga SC, Ramirez MA, Jimenez-Jacinto V, Collado-Vides J, Davila G. Proc Natl Acad Sci U S A 2006;103:3834–9. [PubMed: 16505379]
26. Sambrook, J.; Russell, DW. Condensed Protocols from Molecular Cloning: A Laboratory Manual. Cold Spring Harbor Press; New York: 2006.
27. Brown CM, Dilworth MJ. J Gen Microbiol 1975;86:39–48. [PubMed: 234505]
28. Carson KC, Glenn AR, Dilworth MJ. Arch Microbiol 1994;161:333–339.
29. Emery T. Biochemistry 1965;4:1410–7. [PubMed: 5856641]
30. Lin YM, Miller MJ. Journal of Organic Chemistry 1999;64:7451–7458.
31. Milewska MJ, Chimiak A. Synthesis FIELD Full Journal Title:Synthesis 1990:233–4.
32. Bergeron RJ, Phanstiel OIV. J Org Chem FIELD Full Journal Title:Journal of Organic Chemistry 1992;57:7140–3.
33. Thariath A, Socha D, Valvano MA, Viswanatha T. J Bacteriol 1993;175:589–96. [PubMed: 8423134]
34. Pohlmann V, Marahiel MA. Org Biomol Chem 2008;6:1843–8. [PubMed: 18452021]
35. Sokol PA, Darling P, Woods DE, Mahenthiralingam E, Kooi C. Infect Immun 1999;67:4443–55. [PubMed: 10456885]
36. van Berkel WJ, Kamerbeek NM, Fraaije MW. J Biotechnol 2006;124:670–89. [PubMed: 16712999]
37. Coy M, Paw BH, Bindereif A, Neilands JB. Biochemistry 1986;25:2485–9. [PubMed: 3521734]
38. Trainer MA, Charles TC. Appl Microbiol Biotechnol 2006;71:377–86. [PubMed: 16703322]
39. de Lorenzo V, Bindereif A, Paw BH, Neilands JB. J Bacteriol 1986;165:570–8. [PubMed: 2935523]
40. Chen HP, Lin CF, Lee YJ, Tsay SS, Wu SH. J Bacteriol 2000;182:2052–4. [PubMed: 10715017]
41. Eliot AC, Kirsch JF. Annu Rev Biochem 2004;73:383–415. [PubMed: 15189147]
42. Marahiel MA, Stachelhaus T, Mootz HD. Chem Rev 1997;97:2651–2674. [PubMed: 11851476]
43. Keating TA, Miller DA, Walsh CT. Biochemistry 2000;39:4729–39. [PubMed: 10769129]
44. Challis GL, Ravel J, Townsend CA. Chem Biol 2000;7:211–24. [PubMed: 10712928]
45. Stachelhaus T, Mootz HD, Marahiel MA. Chem Biol 1999;6:493–505. [PubMed: 10421756]
46. Dimise EJ, Widboom PF, Bruner SD. Proceedings from the National Academy of Sciences 2008;105:15311–15316.
47. Santi DV, Webster RW Jr, Cleland WW. Methods Enzymol 1974;29:620–7. [PubMed: 4368856]
48. Payne SM. Methods Enzymol 1994;235:329–44. [PubMed: 8057905]
49. Neilands JB. Science 1967;156:1443–7. [PubMed: 4304945]
50. Lautru S, Oves-Costales D, Pernodet JL, Challis GL. Microbiology 2007;153:1405–12. [PubMed: 17464054]
51. Anke H, Anke T, Diekmann H. FEBS Lett 1973;36:323–5. [PubMed: 4357812]
52. Drechsel H, Jung G. J Pept Sci 1998;4:147–81. [PubMed: 9643626]
53. Sattely ES, Walsh CT. J Am Chem Soc 2008;130:12282–4. [PubMed: 18710233]
54. Challis GL. Microbiology 2008;154:1555–69. [PubMed: 18524911]
55. Krithika R, Marathe U, Saxena P, Ansari MZ, Mohanty D, Gokhale RS. Proc Natl Acad Sci U S A 2006;103:2069–74. [PubMed: 16461464]
56. Visca P, Imperi F, Lamont IL. Trends Microbiol 2007;15:22–30. [PubMed: 17118662]

57. Miller MJ, Zhu H, Xu Y, Wu C, Walz AJ, Vergne A, Roosenberg JM, Moraski G, Minnick AA, McKee-Dolence J, Hu J, Fennell K, Kurt Dolence E, Dong L, Franzblau S, Malouin F, Mollmann U. Biometals 2009;22:61–75. [PubMed: 19130268]

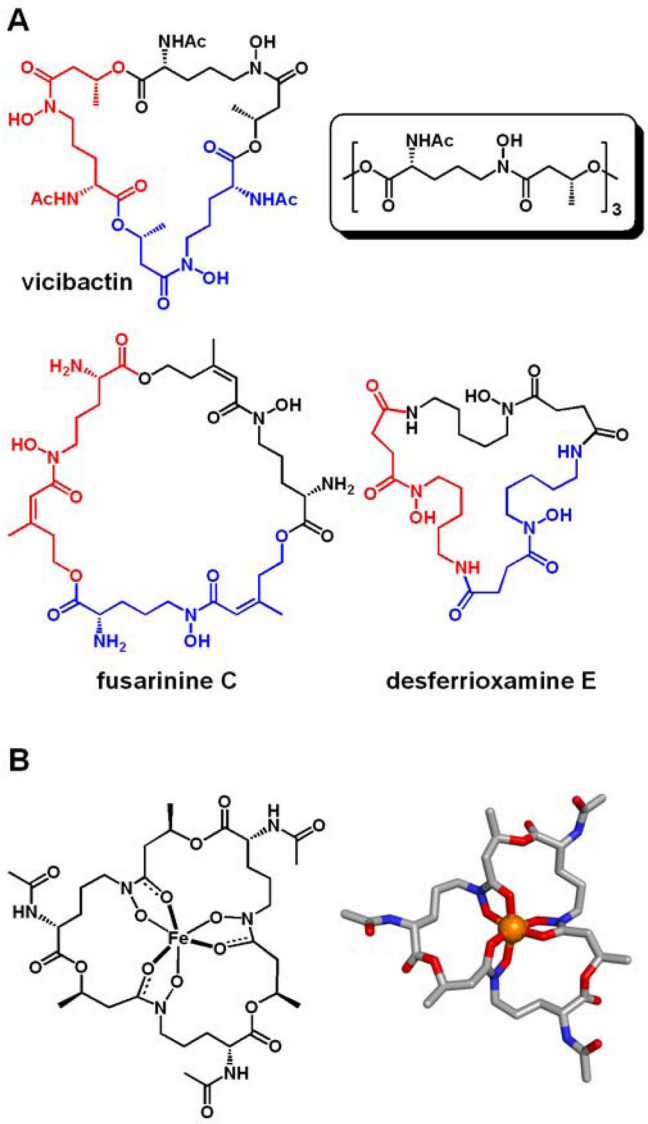

Figure 1.

A. Structures of bacterial (vicibactin and desferrioxamine E) and fungal (fusarinines) trimeric hydroxamate siderophores. **B.** X-ray structure of the neurosporin-Fe complex. Neurosporin, isolated from the fungus, *Neurospora*, is identical to vicibactin.[1]

[1]Neurosporin is a single example of a fungal siderophore containing D-Orn residues; it is also identical in structure to vicibactin.

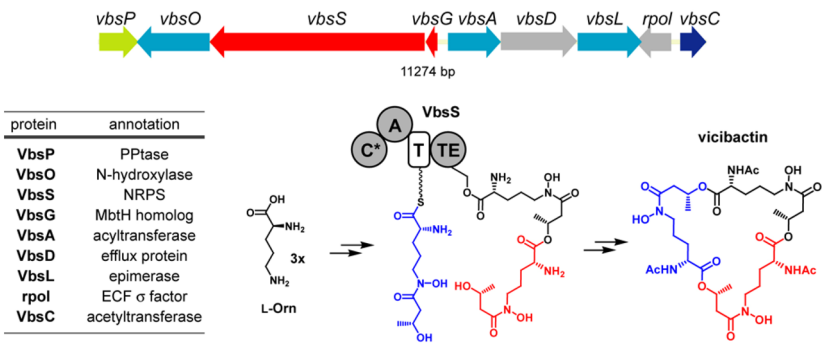

Figure 2.

Vicibactin gene cluster and annotated protein functions. The multidomain NRPS, VbsS, is thought to be the central catalyst responsible for trimerization of the functionalized ornithine monomer. The *N*-terminal condensation domain (marked C*) of VbsS lacks required conserved residues in the active site and is thought to be inactive. (A = adenylation domain, T = thiolation domain, TE = thioesterase domain).

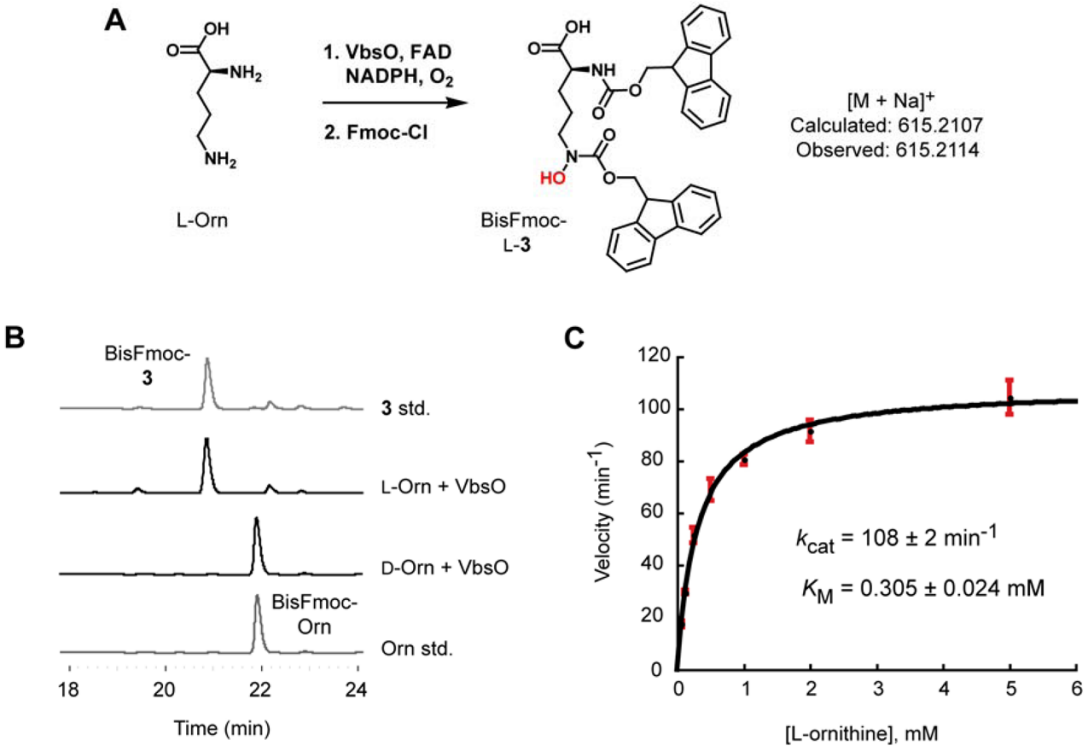

Figure 3.

Characterization of VbsO as an L-ornithine N^5-hydroxylase. (**A**) Schematic of the VbsO-catalyzed conversion of L-Orn to N^5-hydroxy-L-ornithine (L-**3**) and proposed structure of the Fmoc-derivatized product. ESI-HRMS *m*/*z* data of the purified product resulting from incubation of VbsO with L-Orn and subsequent Fmoc-derivatization is consistent with bisFmoc-N^5-hydroxyornithine (bisFmoc-**3**). (**B**) HPLC traces (263 nm) showing the Fmoc-derivatized products resulting from incubation of L- or D-Orn (500 μM) with VbsO (5 μM) in the presence of FAD (50 μM), NADPH (2 mM) and pH 8.0 Tris (50 mM). Peaks corresponding to bisFmoc-Orn appear at t_R 21.9 min and bisFmoc-L-**3** at t_R 20.8 min. (**C**) Plot of initial velocity versus L-Orn concentration, with the best fit curve to the Michaelis-Menten equation. Error bars are drawn at one standard deviation.

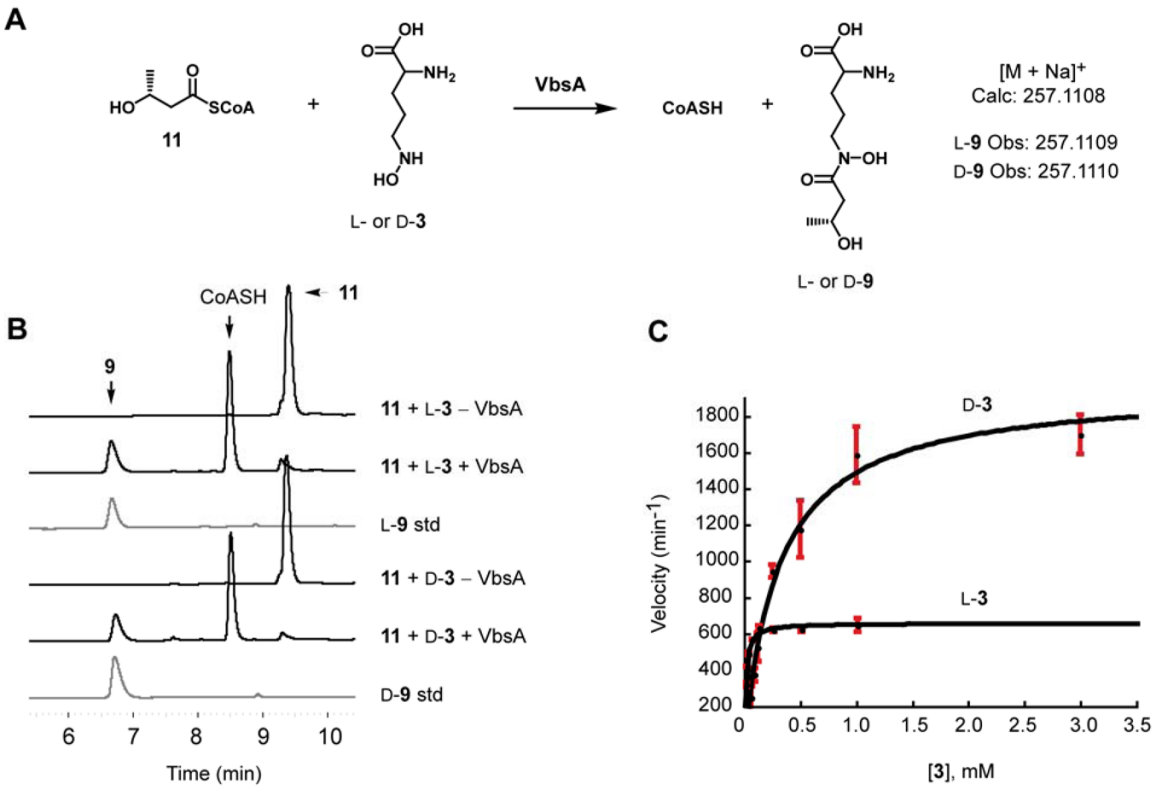

Figure 4.

Characterization of VbsA as a CoA-dependent N^5-hydroxyornithine *N*-((*R*)-3-hydroxybutryl)-transferase. (**A**) Schematic of the VbsA-catalyzed transfer of (*R*)-3-hydroxybutyryl- from the CoA thioester (**11**) to N^5 of N^5-hydroxy-L- or D-ornithine (L- or D-**3**). ESI-HRMS *m*/*z* data of the purified products are consistent with N^5-((*R*)-3-hydroxybutyryl)-N^5-hydroxy-L- and D-ornithine (**9**) (**B**) HPLC traces (220 nm) showing products resulting from the incubation of **11** (1 mM) and L- or D-**3** (1.2 mM) with and without VbsA (1 μM) in pH 7.5 Tris (50 mM). Peaks corresponding to L-**9** appear at t_R 6.6 min, D-**9** at t_R 6.8 min, CoASH at t_R 8.5 min and **11** at t_R 9.4 min. (**C**) Kinetic traces for the VbsA-catalyzed acyltransfer from **11** to L- or D-**3**, with the best-fit curve to the Michaelis-Menten equation. Error bars are drawn at one standard deviation.

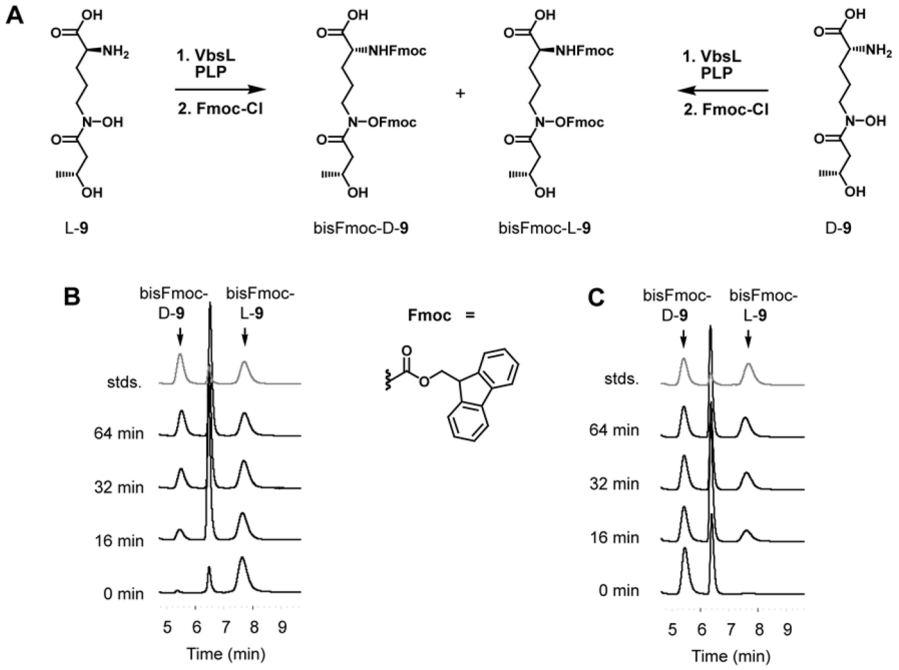

Figure 5.

Characterization of VbsL as a PLP-dependent epimerase. (**A**) Schematic of the VbsL-catalyzed racemization of N^5-((*R*)-3-hydroxybutyryl)-N^5-hydroxy-L- or D-ornithine (L- or D-**9**) and proposed structure of the Fmoc-derivatized products (bisFmoc-L- and D-**9**). (**B**) Chiral HPLC traces (263 nm) showing racemization of L-**9** (1 mM) resulting from incubation with VbsL (500 nM), PLP (50 μM) and pH 7.75 HEPES (50 mM) followed by derivatization with Fmoc-Cl. (**C**) Chiral HPLC traces (263 nm) showing racemization of D-**9** (1 mM) resulting from incubation with VbsL (500 nM), PLP (50 μM) and pH 7.75 HEPES (50 mM) followed by derivatization with Fmoc-Cl. Peaks corresponding to bisFmoc-D-**9** appear at t_R 5.4 min and bisFmoc-L-**9** at t_R 7.6 min. Peak at t_R 6.4 min is an artifact of Fmoc-Cl decomposition in aqueous solution.

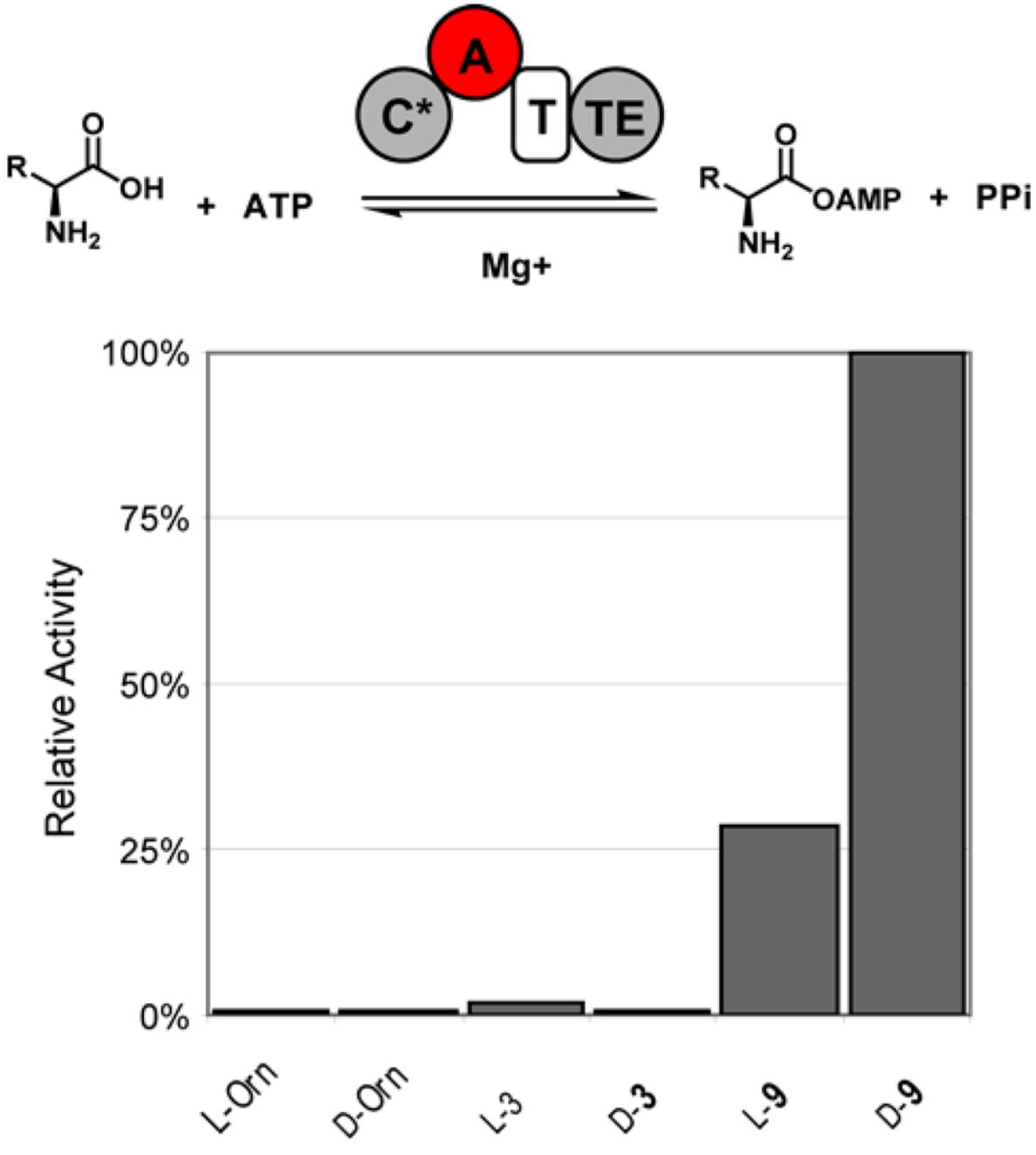

Figure 6.
Relative activities of the VbsS adenylation (A) domain with L- and D-Orn, L- and D-**3** and L- and D-**9** as assessed by ATP-[^{32}P]PPi exchange assays.

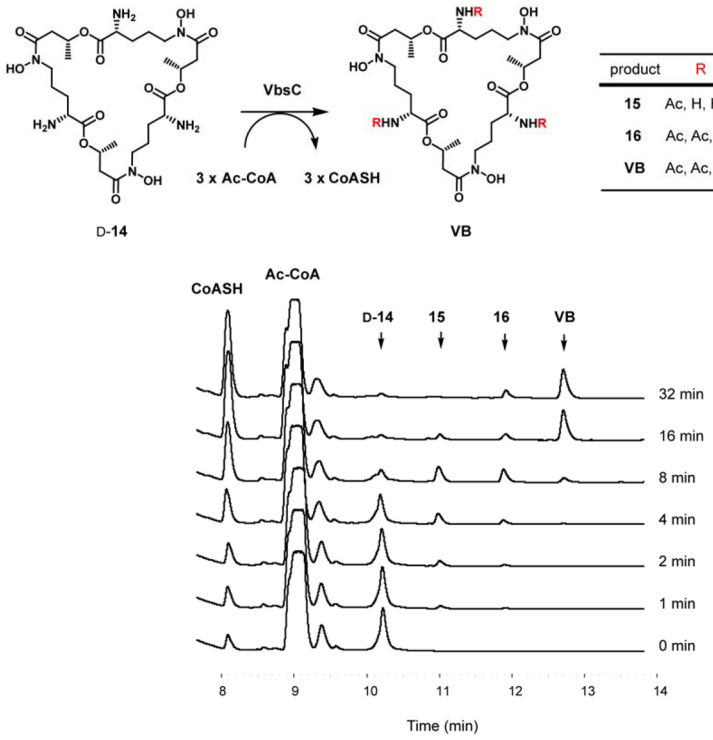

product	R	*m*/z Calc.	Obs.
15	Ac, H, H	691.3509	691.3535
16	Ac, Ac, H	733.3614	733.3622
VB	Ac, Ac, Ac	775.3720	775.3735

Figure 7.

Characterization of VbsC as a CoA-dependent desacetyl-D-vicibactin N^2-acetyltransferase. (**A**) Schematic of the VbsC-catalyzed, tri-acetylation of desacetyl-D-vicibactin (D-**14**) with 3 equivalents of acetyl-CoA and ESI-HRMS *m*/*z* data of purified products. (**B)** HPLC traces (220 nm) showing the time-dependent appearance of mono-, di- and tri-acetylated products resulting from the incubation of D-**14** (1 mM) and acetyl-CoA (4 mM) with VbsC (10 μM) in pH 7.75 HEPES (50 mM). Peaks corresponding to CoASH appear at t_R 8.1 min, Acetyl-CoA at t_R 9.1 min, D-**14** at t_R 10.2 min, monoacetylated D-**15** at t_R 11.0 min, diacetylated D-**16** at t_R 11.9 min and **VB** at t_R 12.8 min.

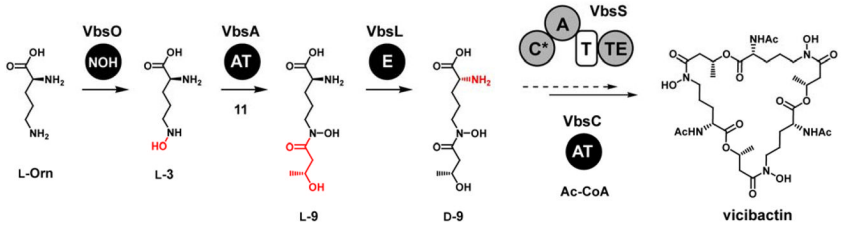

Figure 8.

Logic of vicibactin biosynthesis involves complete functionalization of the Orn-based monomer prior to VbsS catalyzed desacetylvicibactin assembly. Selection for the C^2-D hydroxamate (D-**9**) monomer is maintained by the adenylation (A) domain of VbsS. Tailoring catalyzed by VbsC leads to the fully-functionalized vicibactin siderophore scaffold. (NOH = amine *N*-hydroxylase, AT = acyltransferase, E = epimerase)

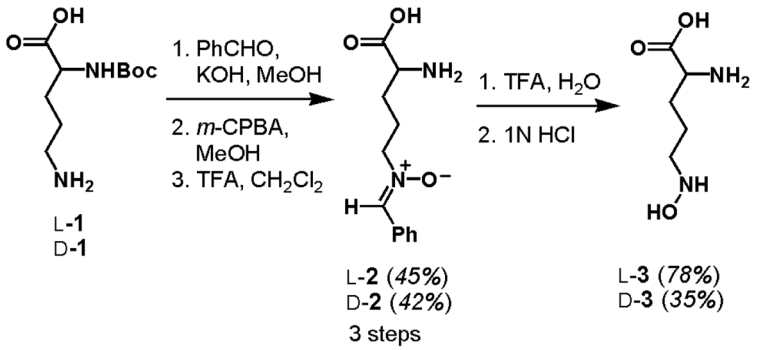

Scheme 1.
Synthesis of hydroxylamines L- and D-**3**. Yields shown in parentheses.

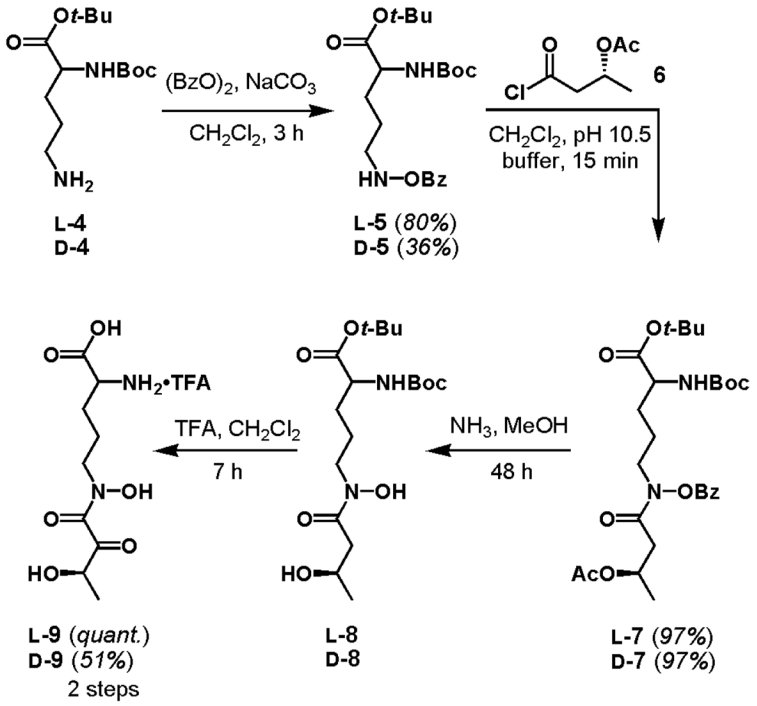

Scheme 2.
Synthesis of hydroxamates D- and L-**9**. Yields shown in parentheses.